Comparisons of the Seismic Properties of the Sun During Solar Cycles 23, 24, and 25

Mike Li, Serena Liu, Jenny Johnson, Agnes Kovesdy, James Wen, Josh Kao, Matthew Steinberger, Dylan Jeninga, Sid Qian, Mowen Zhao, Dongpo Bai
Advisor: Edward Rhodes, Department of Physics and Astronomy, University of Southern California
Collaborators: Charles Baldner and Tim Larson, Stanford University; Johann Reiter, Technical University of Munich; Christopher Toumanian

Abstract

The previous solar activity cycle, Cycle 24, was weaker than Cycles 21, 22, or 23. Because of this weakness in the level of solar activity during Cycle 24, we were interested in learning whether the seismic properties of the solar atmosphere at that time were different from those in Cycle 23. To answer this question, we compared the changes in the frequencies of solar oscillations observed during Cycle 23 with simultaneous changes in seven different indicators of solar activity using 15 years of MDI and GONG oscillation data. We then carried out similar analyses for all of Cycle 24 and the beginning of Cycle 25 using an additional year of HMI data that were not available to us in 2023. We discovered that the sensitivity of the frequency changes to long-term changes in the level of solar activity was reduced significantly by up to 40 percent in Cycle 24 when compared with Cycle 23. We have also extended our analysis through the third year of Cycle 25 and our new results for Cycle 25 are similar to our previous results for Cycle 24. These new results suggest that Cycle 25 will end up being similar, or slightly stronger, in peak strength to Cycle 24, in contrast to some predictions that claimed it would be substantially weaker..

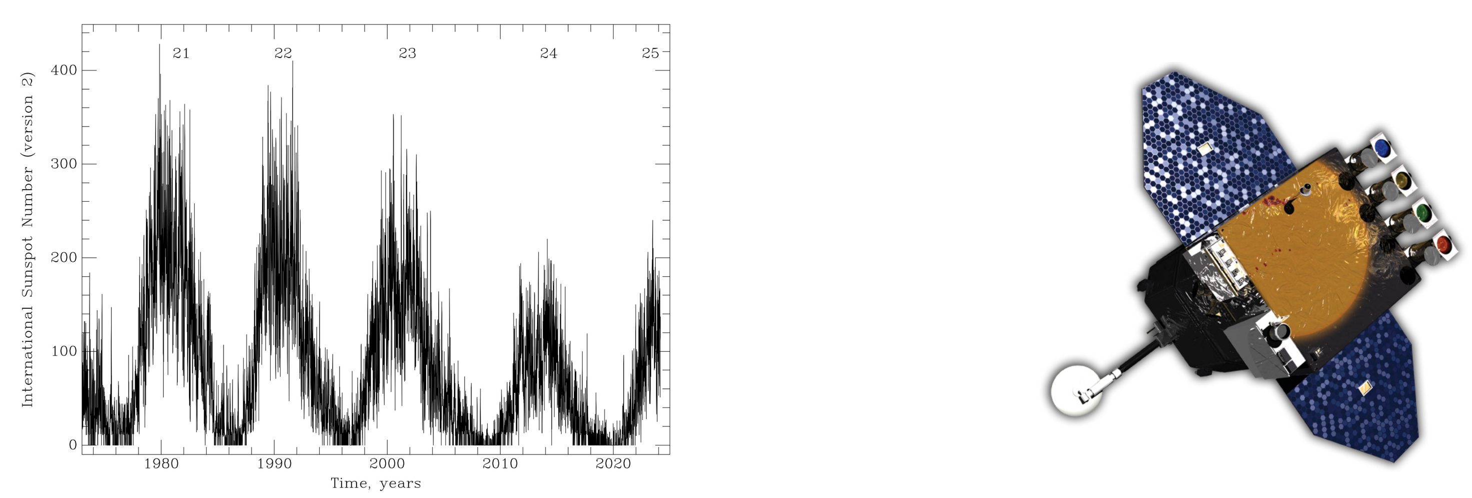

Figure 1:(a) (left): Temporal dependence of the mean International Sunspot Number for Solar Cycles 21 through 25 (to Feb. 29, 2024). A systematic decrease in peak sunspot numbers from Cycle 22 through Cycle 24 is evident. This panel shows that, based upon the International Sunspot Numbers alone, Cycle 25 is now almost as strong as Cycle 24 rather than being weaker. (b) (right): Image of Solar Dynamics Observatory (Courtesy NASA/GSFC)

Purpose

Our project was designed to see if the decline in the peak level of solar activity that began with Cycle 22 also extended into Cycle 25. A better understanding of changes in the seismic properties of the solar atmosphere will help us to better predict future solar activity and space weather.

Method

Our data comes from NASA's Helioseismic and Magnetic Imager (Figure 1b), Michelson Doppler Imager, and GONG+. A total of 1913 3-day time series of dopplergrams were processed by the HMI team at Stanford University, where they were each converted into a set of un-averaged spectra. We transferred the un-averaged spectra to USC and collapsed each of those into a set of 1001 m-averaged spectra. We then fit the peaks in all of the m-averaged spectra from a single 3-day run with the latest version of our Windowed, Multi-Peak, Averaged Spectrum (WMLTP) peak-fitting technique, which fits a set of theoretical profiles to each of the peaks in each m-averaged spectrum. By applying this method to all of the m-averaged spectra from a single run, we obtained a total of 12 288 frequencies, such as those shown in Figure 2a. We also obtained the same number of linewidths, such as those shown in Figure 2b, and the same number of amplitudes, such as those shown in Figure 2c. We next split these tables of fitted parameters into 70 72-day time intervals. We paired all 24 of the tables within each interval and subtracted the corresponding frequencies, linewidths, and amplitudes, generating a total of 276 sets of differences within each interval. One of these sets of frequency differences is shown in Figure 3a. We next binned each set of frequency, width, and amplitude differences into 25 250 μHz-wide bins. The binned frequency shifts that resulted from the raw differences shown in Figure 3a are shown in Figure 3b.

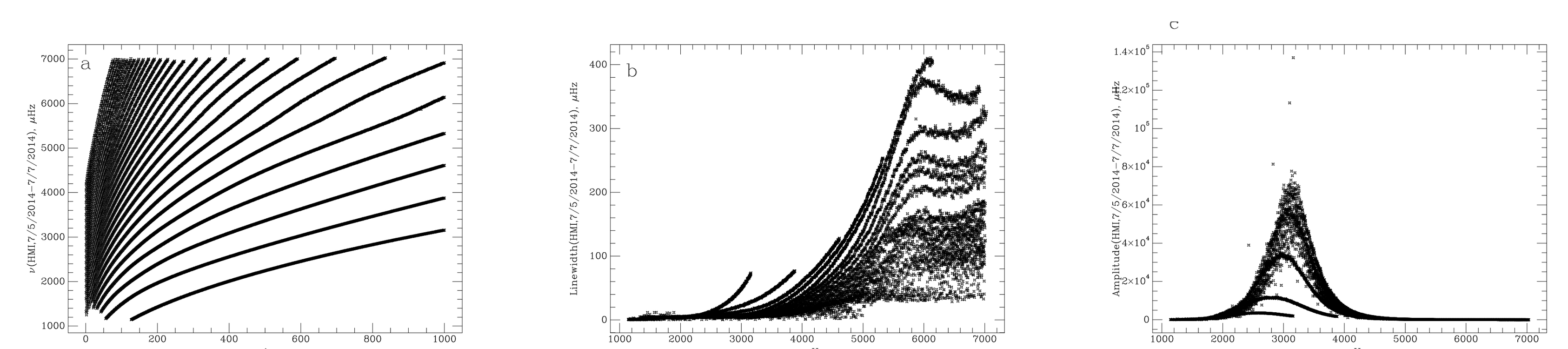

Figure 2:(a) (left): The 12 228 solar oscillation frequencies computed from the HMI observing run of July 5 to July 7, 2014, plotted as a function of the spherical harmonic degree. (b) (center): The frequency dependence of the linewidths of the oscillations computed from the same run. (c) (right): The frequency dependence of the amplitudes of the oscillations computed from the same run.

Data and Results

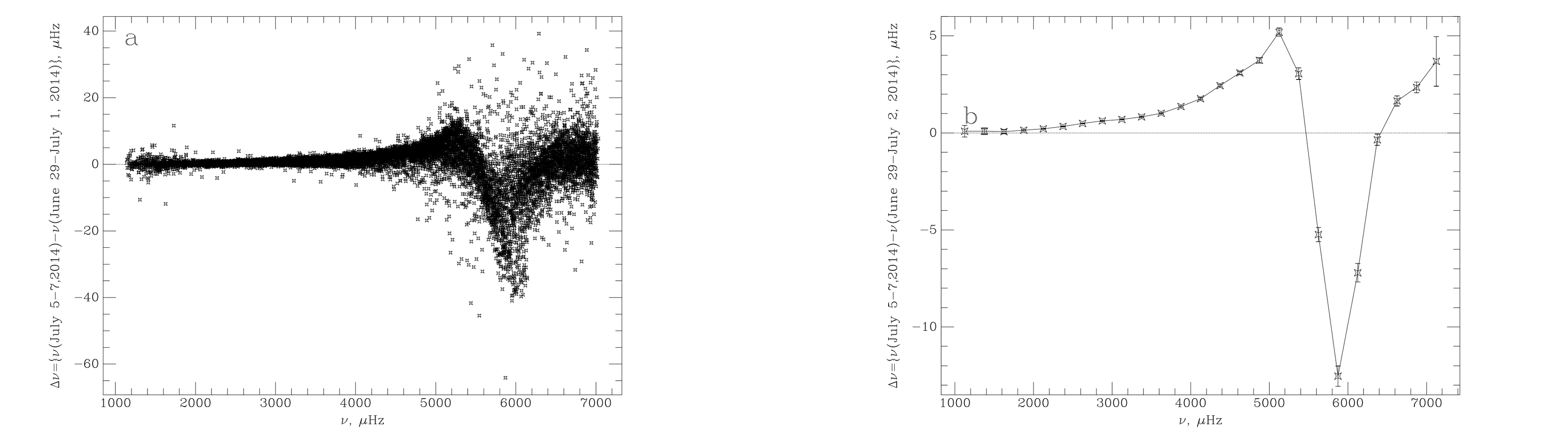

Figure 3:(a) (left): The frequency dependence of the 12 228 differences in the frequencies computed from the July 5 to July 7, 2014 run and the frequencies computed from the June 29 to July 1, 2014 run. (b) (right): The frequency dependence of the 25 binned frequency differences computed from the raw frequency differences shown in panel a. Also shown are the standard errors of each mean frequency. The horizontal dotted line designates frequency differences of 0.0.

We next regressed the 276 binned frequency shifts within each of our 25 bins against differences in 3-day averages of nine different solar activity indices. One example of these regressions for a frequency bin where the frequency shifts were correlated with the activity shifts is shown in Figure 4a. A second example from a higher-frequency bin where the frequency shifts were anti-correlated with the activity differences is shown in Figure 4b.

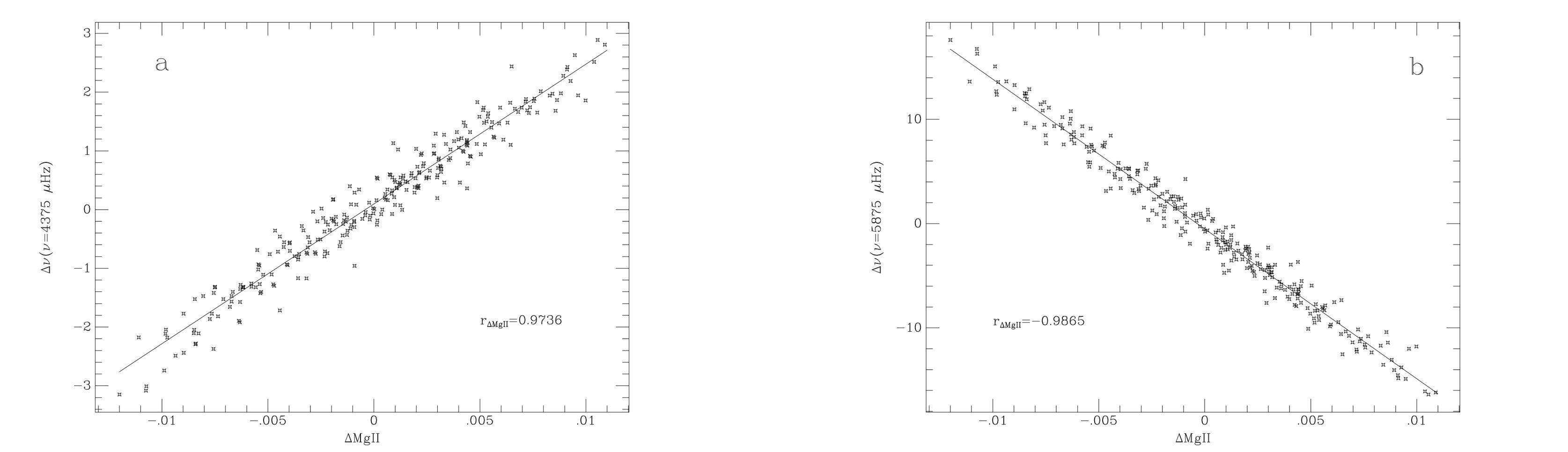

Figure 4:(a) (left): The dependence of the binned frequency differences in the bin centered at $\nu = 4375\,\mu\text{Hz}$ upon the Magnesium 2 Spectra Line (MgII) core-to-wing ratios. The solid line shows the linear regression fit to the 276 data points. The positive slope of this line shows that the frequencies were correlated with the changes in solar activity for this bin. The correlation coefficient $r = 0.9736$, shows that the correlation was strong. (b) (right): The dependence of the binned frequency differences in the bin centered at $\nu = 5875\,\mu\text{Hz}$ upon the MgII core-to-wing ratios. The solid line is the linear regression fit to the 276 data points. The negative slope shows that the frequency were anti-correlated with the changes in solar activity for this bin. The correlation coefficient $r = -0.9865$, shows that the anti-correlation was also strong.

Previous studies of the frequency and linewidth shifts showed systematic signatures in both the slopes and correlation coefficients from similar regression analyses. The signature of the frequency shifts from the first 72-day time interval is shown in Figure 5a. At low frequencies the frequency shifts were correlated with the activity changes, while at intermediate frequencies they became anti-correlated, before once again becoming correlated with the activity changes. We defined the frequency at which the sign of the correlation coefficient changed from positive to negative as $\nu_{+/-}$ and the frequency where it changed back from negative to positive as $\nu_{-/+}$. We show examples of both of these zero-crossing frequencies in Figure 5a.

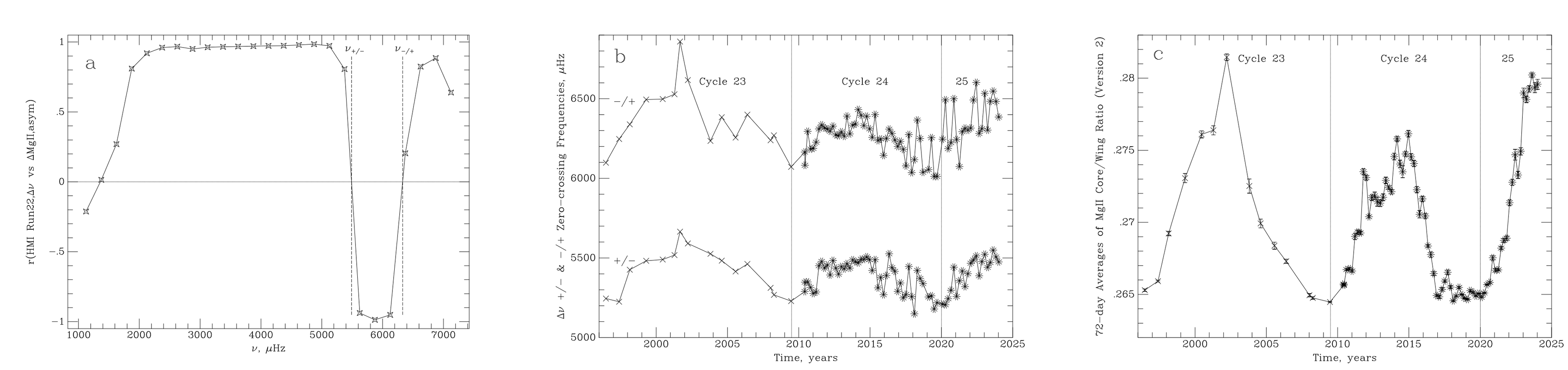

Figure 5:(a) (left): The frequency dependence of the correlation coefficients computed from the 25 linear regression analyses of the binned frequency differences upon the changes in MgII. The left-hand vertical dashed line shows the frequency at which the frequency shifts changed from being correlated with the activity changes to being anti-correlated. This frequency, $\nu_{+/-}$, is designated as the $+/-$ zero-crossing frequency. The right-hand vertical dashed line shows the frequency at which the frequency shifts returned to being positively correlated with the activity differences. This frequency, $\nu_{-/+}$, is designated as the $-/+$ zero-crossing frequency. (b) (center): Plot of both $\nu_{+/-}$ and $\nu_{-/+}$ zero crossings as functions of time in Cycles 23 through the end of the third year of Cycle 25. (c) (right): Plot of the 72 day averages of the MgII Core-to-Wing Ratio over time in Cycles 23, 24, and the first three years of Cycle 25. This panel shows that, in contrast to the International Sunspot Numbers that were shown in Figure 1(a), the MgII Core-to-wing Ratio suggests that Cycle 25 will in fact have a higher peak level of activity than Cycle 24, in contrast to some previous predictions.

The results shown in Figure 5a illustrate the signatures of the short-term temporal variations on a scale of a few days. These short-term signatures were very similar in Cycles 23 and 24. However, we wanted to compare the long-term changes on the scale of an entire solar cycle.

In order to search for such long-term variations, we repeated all of the above steps for 15 time intervals in Cycle 23 and 70 additional 72-day time intervals in Cycles 24 and 25. Both sets of the resulting zero-crossing frequencies are shown as functions of time during both cycles in Figure 5b. Also, the corresponding average values of the MgII Core-to-Wing Ratio solar activity index are shown as a function of time for both cycles in Figure 5c. In order to determine whether the longer-term changes in the frequencies were different in Cycles 23 and 24, we separated our tables of zero-crossings into two smaller tables. The first table contained our MDI zero-crossing frequencies from Cycle 23 (along with a few frequencies from GONG project data in 2001) and the second contained our 47 sets of HMI results from Cycle 24 and one set of MDI results from 2010. We next regressed all of the $+/-$ frequencies and all of the $-/+$ frequencies in the first table against the average values of the MgII index during each of the 15 observing runs. We then regressed all of the $+/-$ frequencies and all of the $-/+$ frequencies in the second table against the average values of the MgII index during each of those 48 observing runs. All four of these long-term regression fits are shown in the four panels of Figure 6. To test the statistical significance of the differences in the intercepts and slopes of our two pairs of regression fits, we employed the statistical tests described in **"Applied Regression Analysis and Other Multivariable Methods"** by Kleinbaum and Kupper (1978). We found that the intercepts and slopes of the two $-/+$ regression analyses differed significantly at the 98% confidence level, while the intercepts and slopes of the two $+/-$ analyses differed at the 78% confidence level. For example, the $-/+$ slope in Cycle 24 was equal to only 60% of the $-/+$ slope in Cycle 23, while the $+/-$ slope in Cycle 24 was equal to 75% of the slope in Cycle 23.

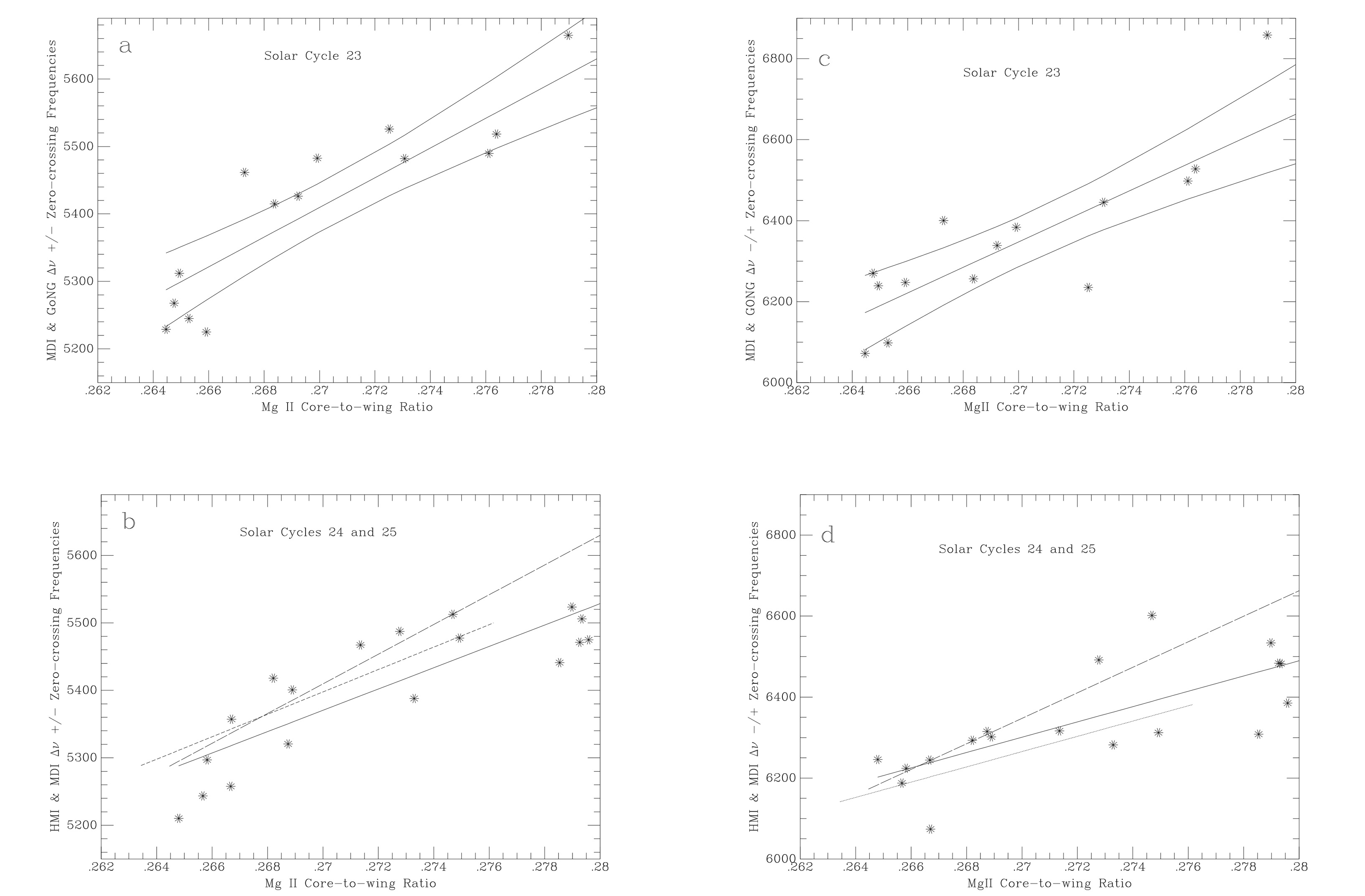

Figure 6:(a) (upper-left): Dependence of the $+/-$ zero-crossing frequencies measured during Cycle 23 as a function of the average MgII Core-to-wing Ratio, an index of solar activity. (b) (lower-left): Same as panel a except runs from Solar Cycles 24 and 25 are shown. 19 of the 21 $+/-$ zero-crossing frequencies from Cycle 25 are shown as the asterisks. The dashed line is the fit form Cycle 23 from panel a, while the dotted line is the fit for Cycle 24, and the solid line is the fit for Cycle 25. (c) (upper-right): Same as panel a except that here the $-/+$ zero-crossing frequency shifts were plotted. (d) (lower-right): Same as panel c except runs from Solar Cycles 24 and 25 are shown. 19 of the 21 $-/+$ zero-crossing frequencies from Cycle 25 are shown as the asterisks. The other two $-/+$ frequencies were outliers which are not included here. The dashed line is the fit for Cycle 23 from panel c, while the dotted line is the fit for Cycle 24, and the solid line is the fit for Cycle 25. We see statistically-significant differences in the slopes and intercepts of the $-/+$ regression fits for Cycles 23 and 24 at the 98 percent confidence level and of the $+/-$ fits at the 78 percent level.

Conclusions

The signatures of the short-term variations in the frequencies of the solar oscillations were very similar in both Solar Cycles 23 and 24. However, the long-term sensitivity of both sets of zero-crossing frequencies to changes in the MgII activity index was reduced during Cycle 24 by up to 40% from Cycle 23. We have also extended our long-term analysis through the 4th year of Cycle 25, and our new results for Cycle 25 are very similar to those of Cycle 24. These new regression lines are consistent with the similar peak strength of Cycles 24 and 25 that we showed in Figure 1(a). We believe that these changes in long-term sensitivity of the frequency shifts were likely due to corresponding structural changes in the low solar atmosphere during these three cycles. Our new results should spur future theoretical analyses of the seismic structure of the solar atmosphere.